

Photocatalytic Degradation and Reaction Pathway Studies of Chlorinated Hydrocarbons in Gaseous Phase

W.A.W. Abu Bakar^{1,*}, R. Ali¹ and M.Y. Othman¹

Abstract. *TiO₂ was doped with various types of first row transition metals towards the degradation of dichloromethane, chloroform, carbon tetrachloride and a mixture of carbon tetrachloride and chloroform. Zn²⁺/Fe³⁺/TiO₂ photocatalyst with the ratio of 0.0005: 0.0005: 1 was revealed as the best catalyst in this study. 41.05% of dichloromethane, 49.45% of chloroform and 37.84% of carbon tetrachloride were degraded by this catalyst in the presence of UV light (6 W, 354 nm), irradiated for 90 minutes, and oxidized VOCs gases were analyzed using GC-FID. In this study, the new species of CHCl₂⁺, CH₂Cl⁺, CCl₂⁺ and OCl⁺. CHCl₂⁺ was detected to form from the photocatalytic degradation of chloroform while some new fragments, such as OCl⁺, CHCl₂⁺ and CH₂Cl⁺, are observed during the photocatalytic degradation of carbon tetrachloride.*

Keywords: *Photocatalyst; Dichloromethane; Chloroform; Carbon tetrachloride titanium dioxide; Chlorinated hydrocarbon; mineral components.*

INTRODUCTION

Photocatalytic oxidation (PCO) harnesses radiant energy from natural or artificial light sources with a heterogeneous catalyst to degrade the organic pollutants into their mineral components. In recent years, photocatalytic oxidation of organic compounds in the gaseous-phase using TiO₂ as a catalyst appears to be a promising process for the remediation of ground water and air polluted by Volatile Organic Hydrocarbons (VOC). The high degree of recombination between photogenerated electrons and holes is a major limiting factor controlling the photocatalytic efficiency [1]. In this case, the deposited metal on the surface of TiO₂ can act as a sink for a photoinduced charge carrier promoting an interfacial charge transfer process.

Brezova et al. [2] found that the best results for the photodegradation of phenols were obtained

on dopant free TiO₂, Li⁺/TiO₂, Zn²⁺/TiO₂ and Pt⁰/TiO₂ catalysts. Recently, some research has co-doped transition metals such as Fe³⁺ with Zn²⁺ into TiO₂ [3]. It was found that co-doped TiO₂ shows better degradation of phenol than metal doped TiO₂. Navio et al. [4] reported that Fe(NO₃)₃·9H₂O containing low amounts of Fe³⁺ ions are more efficient for nitrite oxidation than pure TiO₂. The photocatalytic degradation of carboxylic acid by Fe³⁺-doped TiO₂ had been studied by Arana et al. [5]. It was revealed that all catalysts calcined at 773 K are able to totally degrade formic acid after 1.5 hours in reaction. Arroyo et al. [6] found out that the transformation of anatase to rutile depends significantly on Mn²⁺ concentration and it seemed that the dopant segregation occurs for Mn²⁺ concentration up to 1.5 mol%, which is responsible for the acceleration of the anatase-rutile transformation. An increase in the degradation activity of phenol by 1-2 times is observed in the case of co-doping Zn²⁺ and Fe³⁺ with TiO₂. The maximum photocatalytic activity occurred at the concentration of approximately 0.5 mole% Zn²⁺ and 1 mole% Fe³⁺ above which the co-doping had a reduced and eventually detrimental effect on the activity. The maximum photodegradation

1. Department of Chemistry, Faculty of Science, Universiti Teknologi Malaysia, 81310 UTM Skudai, Johor, Malaysia.

*. Corresponding author. E-mail: wanazelee@yahoo.com

Received 28 April 2009; received in revised form 8 August 2009; accepted 19 October 2009

of chloroform in solution using TiO_2 co-doped with Fe^{3+} and Eu^{3+} is more than 5 times compared with the one produced by pure nanocrystalline TiO_2 . In nanocrystalline TiO_2 , there are cooperative actions of the 2 dopants where Fe^{3+} is served as hole trap while Eu^{3+} is served as an electron trap [7]. Feiyen et al. [8] investigated that the VOCs degrade in air following first-order kinetics in the range of 80-500 ppm. However, when the initial concentration of chloroform is higher than 600 ppm, the reaction seems to follow second-order kinetics, with respect to chloroform concentration.

So far, research in photocatalysts mostly focused on the degradation of organic compounds in the aqueous system, such as organic compounds (Pd^{2+} , $\text{Cu}^{2+}/\text{TiO}_2$), methyl dyes ($\text{Fe}^{3+}/\text{TiO}_2$), Rhodamine B ($\text{Fe}^{3+}/\text{TiO}_2$) and carboxylic acid or fatty acid ($\text{Fe}^{3+}/\text{TiO}_2$). Only a few studies have been published which consider the photocatalytic degradation of gaseous VOCs using doped TiO_2 . As such, the present investigation is directed to degradation of some volatile organic compounds, eg. dichloromethane, chloroform and carbon tetrachloride, in the gaseous phase.

EXPERIMENTAL

Catalyst Preparation

TiO_2 sol-gel was prepared by modification of the sol-gel method reported by Kato et al. [9]. 6 g of polyethylene glycol (PEG) (2000) were dissolved in 600 mL ethanol. 85.2 g titanium tetraisopropoxide, 31.8 g diethanolamine and 5.4 mL deionized water were added to the solution. For preparation of a catalyst with dopants, the metal salt was weighed based on the required amount, and dissolved with 135 mL sol-gel. The mixture was stirred till homogeneous. The sol-gel was then used to prepare TiO_2 thin films. A hollow pyrex glass cylinder was used as the support substrate. The TiO_2 thin film was prepared by the dip-draw method for 5 times to get a homogeneous thin film on the support. After that, the thin film was dried in the oven at 80°C for 1 hour. Finally, it was calcined with an elevated temperature of $2^\circ\text{C}/\text{min}$, up to 500°C for 1 hour.

Photocatalytic Activity Testing

All photocatalytic degradation experiments of dichloromethane, chloroform and carbon tetrachloride were conducted in a home built fixed bed annulus glass reactor with exactly 100 mL. The reactor was equipped with an electromagnetic pump to circulate the sample, a glass compartment to place the catalyst, and a UV light with wavelength of ~ 354 nm.

Reactor effluent was analyzed every 10 minutes for 90 minutes using GC-FID. All experiments were carried out under atmospheric pressure and at room temperature ($28-30^\circ\text{C}$). For the mechanistic study, a Hewlett-Packard System 5890 Series II GC and 5989 MS were used to analyze fragments that may form during the photocatalytic degradation of the VOCs. A mixture of CHCl_3 and CCl_4 with a ratio of 1.09: 1 was used as the low concentration mixture and 1.24: 1 as the high concentration mixture for the testing.

Catalyst Characterization

The absorption spectrum for metal ions doped TiO_2 and undoped TiO_2 was recorded by a UV-Vis-NIR Shimadzu UV-3101 PC Spectrophotometer in the wavelength range of 300-540 nm. The surface morphology of the potential catalyst was characterized using a Philip XL 40 Microscope with magnification of 5000 and 30 kV scanning voltage. XRD analysis was done by using a diffractometer D5000 Siemens Crystalloflex with CuK_α radiation ($\lambda = 1.54060 \text{ \AA}$). Scans were performed in a step mode of 0.20 seconds/step. The data obtained was analyzed by a PC interfaced to the diffractometer using software called Diffrac Plus. The results were then compared with the accumulated Powder Diffraction File (PDF) data which comes with the software used in this technique.

RESULTS AND DISCUSSION

Photocatalytic Degradation of Dichloromethane, Chloroform and Carbon Tetrachloride

Table 1 depicts the percentage degradation of dichloromethane, chloroform and carbon tetrachloride catalyzed by doped and undoped TiO_2 catalyst. $\text{Zn}^{2+}/\text{Fe}^{3+}/\text{TiO}_2$ catalyst with the ratio of 0.0005: 0.0005: 1 shows the best degradation activities compared to other metals-doped TiO_2 and pure TiO_2 catalysts. In the photocatalytic degradation process, a good dopant must be able to act as both the electron and hole trap, so that the recombination process between photogenerated electrons and holes can be suppressed. It is believed that there is a synergistic effect in photocatalytic activity when both Fe^{3+} and Zn^{2+} metal ions were co-doped into TiO_2 . The effect may be explained by the cooperative operation of the Fe^{3+} and Zn^{2+} in trapping charge carriers and mediating the interfacial charge transfer process. Zn^{2+} and Fe^{3+} dopants in TiO_2 can be randomly dispersed on the TiO_2 surface in the form of their oxides [3]. Due to the difference in the energy band position, the dispersed oxides on the TiO_2 surface will involve

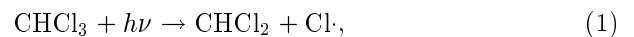
Table 1. Percentage degradation of dichloromethane, chloroform and carbon tetrachloride using doped and pure TiO₂ catalysts for 90 minutes.

Catalysts	Dopant Ratios	% Degradation		
		CH ₂ Cl ₂	CHCl ₃	CCl ₄
Mn ²⁺ /TiO ₂	0.0003: 1	11.95	13.06	10.94
	0.0005: 1	16.47	19.57	15.87
	0.001: 1	11.49	13.12	12.12
Fe ²⁺ /TiO ₂	0.0003: 1	22.08	29.08	13.42
	0.0005: 1	33.79	34.21	20.80
	0.001: 1	22.76	30.84	12.36
Fe ³⁺ /TiO ₂	0.0003: 1	34.53	35.74	22.07
	0.0005: 1	36.02	43.10	35.42
	0.001: 1	33.91	35.11	24.44
Zn ²⁺ /TiO ₂	0.0003: 1	34.01	34.43	22.77
	0.0005: 1	34.89	36.98	27.44
	0.001: 1	33.98	34.77	23.32
Cu ²⁺ /TiO ₂	0.0003: 1	31.84	34.27	22.46
	0.0005: 1	34.30	36.14	25.67
	0.001: 1	32.81	34.45	23.07
Zn ²⁺ /Fe ³⁺ /TiO ₂	0.0003: 0.0005: 1	34.27	36.55	32.89
	0.0005: 0.0005: 1	41.05	49.45	37.84
	0.0005: 0.001: 1	34.06	39.02	32.73
Cu ²⁺ /Fe ³⁺ /TiO ₂	0.0003: 0.0005: 1	31.87	36.11	24.10
	0.0005: 0.0005: 1	36.76	42.55	33.88
	0.0005: 0.001: 1	33.56	38.63	31.03
Pure TiO ₂	–	20.93	23.87	17.40

some charge transfer between them and TiO₂ during illumination. The valence band of TiO₂ is lower than Fe₂O₃, so, the photogenerated holes can move into ZnO, while the photogenerated electrons can move into Fe₂O₃.

From Table 1, the rate of degradation of the studied chlorinated hydrocarbons follows the order: CHCl₃ > CH₂Cl₂ > CCl₄. It is reported that chloroform will show Cl-sensitized degradation when its concentration is above 500 ppm [8]. The concentration of chloroform that was used in the photocatalytic degradation process is more than 500 ppm. Hence, the degradation of chloroform is expected to undergo

Cl-sensitized degradation (Equations 1 and 2)



Since dichloromethane has two chlorine atoms in its structure, Cl-sensitized degradation is lower than in the degradation of chloroform, which has three chlorine atoms in its structure. Therefore, dichloromethane shows lower levels of degradation than chloroform. Carbon tetrachloride shows the lowest levels of degradation in this study. Carbon tetrachloride is a stable

compound, thus, chlorine radicals do not attack the C-Cl bond and, hence a Cl-sensitized degradation does not happen in CCl₄.

In a real industrial application, chlorinated VOCs are found in nature. Therefore, photocatalytic degradation of chloroform and carbon tetrachloride mixtures has been carried out using a Zn²⁺/Fe³⁺/TiO₂ catalyst. The initial concentration of chloroform used in the photocatalytic degradation is 222 ppm for low and 528 ppm for high concentrations of chloroform. Meanwhile, the initial concentration of carbon tetrachloride used is 203 ppm for low concentration and 427 ppm for high concentrations of the mixture. It is noted that 50.89% and 43.87% of chloroform and carbon tetrachloride were degraded, respectively, at 90 minutes for low concentrations of mixture (chloroform: carbon tetrachloride = 1.09: 1). However, for high concentrations of mixture (chloroform: carbon tetrachloride = 1.24: 1), only 43.85% and 35.32% of chloroform and carbon tetrachloride were degraded, respectively, at 90 minutes. This indicates that the amount of chloroform and carbon tetrachloride being degraded depends on the amount of hydroxyl radicals on the catalyst, which, in turn, depends on the number of holes generated on the catalyst. With a higher concentration of chloroform and carbon tetrachloride mixture, the generated hydroxyl radicals are insufficient to degrade the chloroform and carbon tetrachloride.

According to Figure 1, the degradation of chloroform is higher than carbon tetrachloride. During illumination using the UV lamp (6 W, λ = 354 nm), Cl-radicals are formed, since the mixture contained chloroform and carbon tetrachloride. The Cl-radicals do not attack C-Cl bonds in carbon tetrachloride. Therefore, Cl-radicals formed during the illumination of the UV lamp may contribute to the degradation

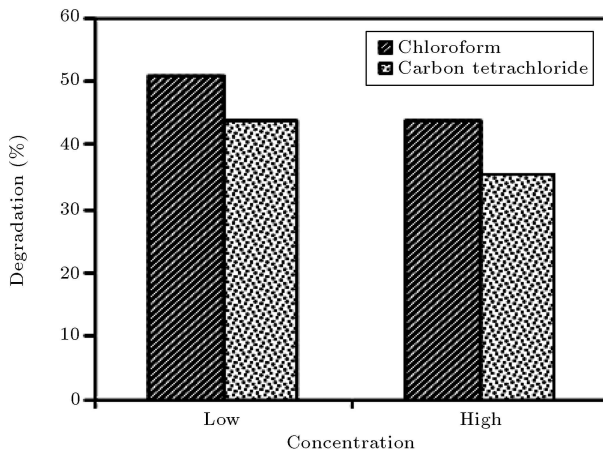
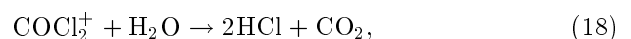
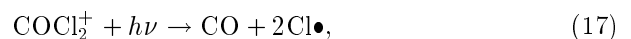
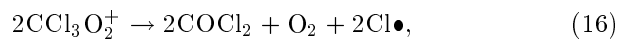
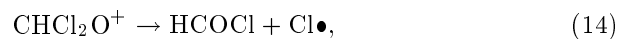
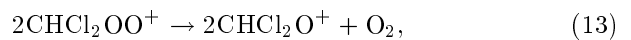
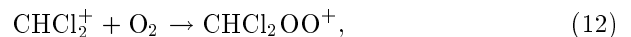
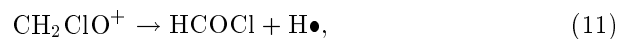
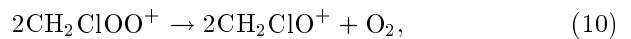
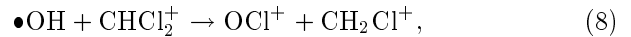
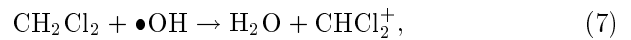
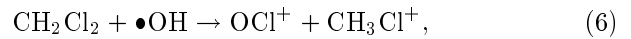
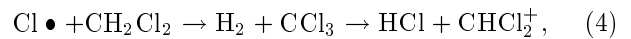
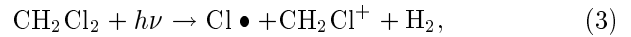


Figure 1. Percentage degradation of chloroform/carbon tetrachloride mixture at 90 minutes using Zn²⁺/Fe³⁺/TiO₂ as catalyst.

of chloroform. Consequently, more chloroform was degraded.

Reaction Pathway for the Photocatalytic Degradation of Chlorinated Hydrocarbons Using Zn²⁺/Fe³⁺/TiO₂ Photocatalyst; UV λ = 354 nm for 90 Minutes

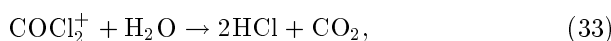
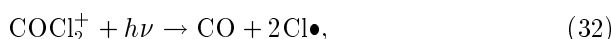
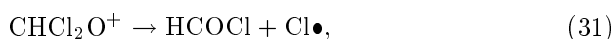
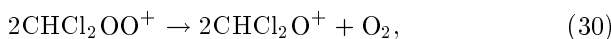
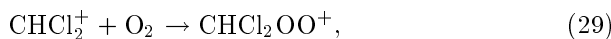
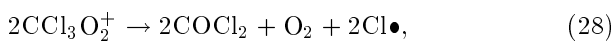
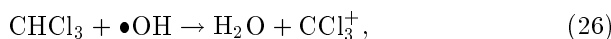
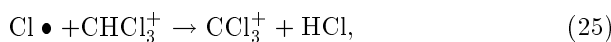
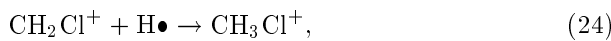
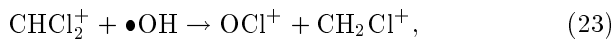
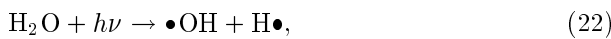
When photocatalytic degradation of VOCs was conducted, the information obtained from the use of GC-MS was used to predict the possible reaction pathway of the photocatalytic degradation process. Fragments obtained before and after illumination of the UV light for dichloromethane, using Zn²⁺/Fe³⁺/TiO₂ as catalyst and analyzed using GC-MS, are depicted in Appendices A and B. A model for the photocatalytic degradation of dichloromethane is proposed as follows:



Chlorine radicals were formed during the illumination

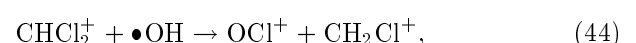
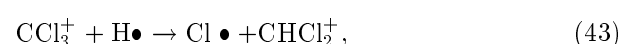
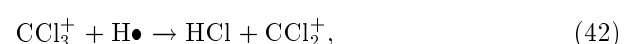
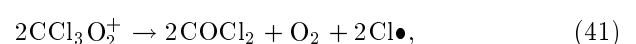
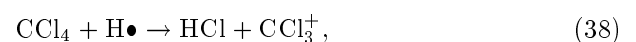
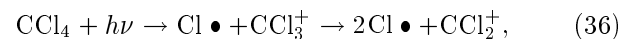
of CH_2Cl_2 using UV light. Chlorine radicals are expected to attack dichloromethane to initialize the degradation process (Equation 3). Besides that, $\bullet\text{OH}$ will attack dichloromethane to form OCl^+ and CH_3Cl^+ through Equation 6 or H_2O and dichloromethane through Equation 7. In the photocatalytic degradation of dichloromethane, it is expected that CCl_3^+ will react with O_2 to form CCl_3O_2^+ (Equation 15). However, CCl_3O_2^+ is not detected in this study. This may be due to the formation of fragments and their fast reaction time, which renders them unable to be detected. COCl_2^+ formed from CCl_3O_2^+ is expected to undergo photolysis (Equation 18) in the presence of moist air. In the termination process, $\text{Cl}\bullet$ will recombine to form Cl_2 (Equation 19), while $\text{H}\bullet$ will combine with $\bullet\text{OH}$ to form H_2O (Equation 20). In this study, only a small amount of phosgene was detected. This may be due to the COCl_2^+ formed during the photocatalytic degradation process, which is expected to undergo photolysis (Equation 18).

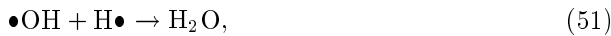
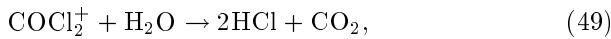
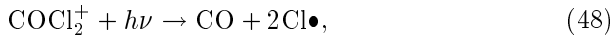
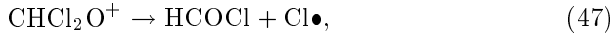
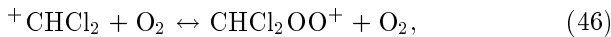
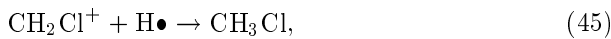
In a case of chloroform, the fragments obtained before illumination of UV light for dichloromethane, using $\text{Zn}^{2+}/\text{Fe}^{3+}/\text{TiO}_2$ as catalyst and analyzed by using GC-MS are shown in Appendices C and D. A possible reaction pathway for the photocatalytic degradation of chloroform is as follows:



A previous research conducted by Feiyen et al. [8] about photodegradation of chloroform and carbon tetrachloride with no catalyst using a low mercury lamp obtained 92% degradation at 254 nm and 6% at 185 nm and observed fragments such as CHCl_2^+ , CCl_3^+ , CCl_3O_2^+ , CHCl_2OO^+ and CHCl_2O^+ . In the presence of UV light with ~ 354 nm, the photocatalytic degradation of chloroform results in the formation of $\text{Cl}\bullet$ and CHCl_2^+ . Then, $\text{Cl}\bullet$ and CHCl_2^+ will decompose into CCl_2^+ and HCl (Equation 21). The fragments which are not observed in the research done by Feiyen, but which are observed in this study, are CHCl_2^+ , CH_2Cl^+ , CCl_2^+ and OCl^+ . CHCl_2^+ formed from the photocatalytic degradation of chloroform can react with $\bullet\text{OH}$ to form CH_2Cl^+ (Equation 23). CH_2Cl^+ reacts with $\text{H}\bullet$ to form CH_3Cl^+ through Equation 24. When chloroform is degraded, it will not only be attacked by $\text{Cl}\bullet$ but also $\bullet\text{OH}$ to form H_2O and CCl_3^+ (Equation 26). Similar to the photodegradation of CH_2Cl_2 , CCl_3O_2^+ that is expected to form from the reaction between O_2 and CCl_3^+ through Equation 27 is also not observed in this study. Phosgene formed from CCl_3O_2^+ is expected to undergo hydrolysis, since the photocatalytic degradation of chloroform was carried out under ambient conditions, which contain moist air, as has similarly been reported [8] as a prerequisite for the process of phosgene photolysis.

Fragments such as CCl_3^+ , CCl_2^+ and CCl_3O_2^+ were observed by Feiyen et al. [8] during the photodegradation of carbon tetrachloride. In this study, some new fragments such as OCl^+ , CHCl_2^+ and CH_2Cl^+ were also observed. The fragments obtained before and after illumination of UV light for carbon tetrachloride, using $\text{Zn}^{2+}/\text{Fe}^{3+}/\text{TiO}_2$ as catalyst and analyzed by using GC-MS, are given in Appendices E and F. As such, the new reaction pathway proposed is as follows:





Chlorine radicals formed in the presence of UV light will not attack the C-Cl bond in carbon tetrachloride, hence, chlorine radicals sensitized degradation does not happen in the case of carbon tetrachloride [8]. During the illumination of UV, the produced $\text{Cl}\bullet$ will react with CCl_3^\bullet to form $\text{Cl}\bullet$ and CCl_2^\bullet (Equation 36). Carbon tetrachloride can be attacked by $\bullet\text{OH}$ to form HCl and CCl_3^\bullet (Equation 38). CCl_3^\bullet produced in the photocatalytic degradation of carbon tetrachloride can react with O_2 to form $\text{CCl}_3\text{O}_2^\bullet$ (Equation 40) or react with $\text{H}\bullet$ to produce CCl_2^\bullet and CHCl_2^\bullet (Equations 42 and 43). However, in this study, $\text{CCl}_3\text{O}_2^\bullet$ is unable to be detected. Similar to previous cases, $\text{CHCl}_2\text{OO}^\bullet$ is unable to be detected. Since the presence of $\text{CHCl}_2\text{O}^\bullet$ is able to be identified by GC-MS, $\text{CHCl}_2\text{OO}^\bullet$ is presumed to be present in the photocatalytic degradation of carbon tetrachloride. A small amount of phosgene is also detected because it is rapidly hydrolyzed to CO_2 and HCl in the presence of moisture.

Characterization of Catalyst

UV-Vis Spectroscopy

A higher wavelength or red shift is noted for $\text{Zn}^{2+}/\text{Fe}^{3+}/\text{TiO}_2$ catalyst compared to the pure TiO_2 (Figure 2). This indicates a decrease in the band gap value of the respective catalyst. This catalyst also has higher absorbance than the pure TiO_2 catalyst in the visible region. The red shift in the optical energy gap is considered to be due to the energy level for dopants, which lies below the conduction band edge (E_{cb}) and above the valence band edge (E_{vb}) of TiO_2 . The introduction of such energy levels in the band gap induces the red shift in the band gap transition and the visible light absorption through a charge transfer between a dopant and cb (or vb) or a $d-d$ transition in the crystal field, according to the energy level. Jiang and Gao [10] had also found out that an addition of Fe^{3+} into TiO_2 had shifted the absorption edge to a higher wavelength.

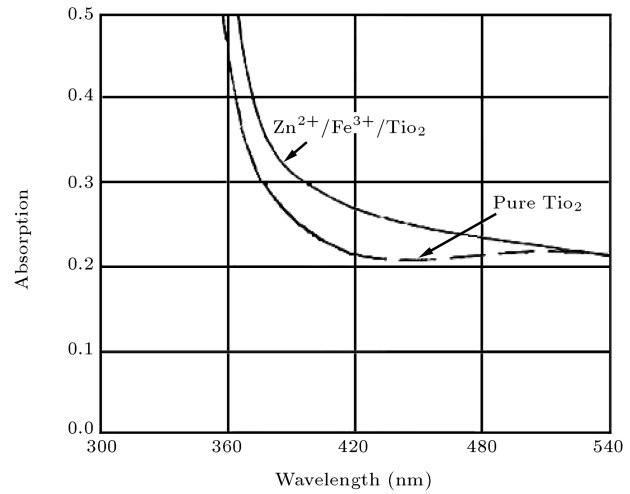


Figure 2. UV-Vis absorption spectra for $\text{Zn}^{2+}/\text{Fe}^{3+}/\text{TiO}_2$ catalyst and pure TiO_2 thin film.

Scanning Electron Microscope (SEM)

Figure 3 shows the SEM micrograph of $\text{Zn}^{2+}/\text{Fe}^{3+}/\text{TiO}_2$ thin film. It was found that pores are produced on the thin film. Pores are produced because PEG contained in the sol-gel decomposes at 450°C [11]. In the preparation of $\text{Zn}^{2+}/\text{Fe}^{3+}/\text{TiO}_2$ thin film, PEG was added into the sol-gel and the catalyst was calcined at 500°C . Therefore, it is expected that pores exist in the catalyst and this result is in a good agreement with the obtained micrograph.

Powder X-Ray Diffraction (XRD)

Figure 4 illustrates the diffractogram of a commercial TiO_2 anatase structure and the prepared catalyst of $\text{Zn}^{2+}/\text{Fe}^{3+}/\text{TiO}_2$ (0.0005:0.0005:1) taken in the powdery form for comparison. It is obvious that the prepared $\text{Zn}^{2+}/\text{Fe}^{3+}/\text{TiO}_2$ catalyst possesses an anatase structure. However, the peaks due to the dopants were not detected and this could be explained

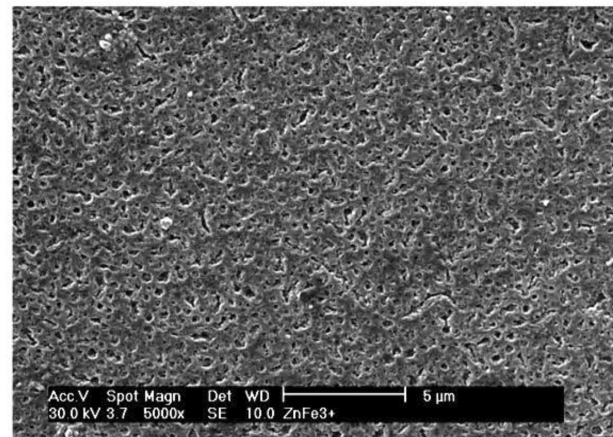


Figure 3. SEM micrograph of Zn^{2+} co-doped $\text{Fe}^{3+}/\text{TiO}_2$ with magnification of $5000\times$.

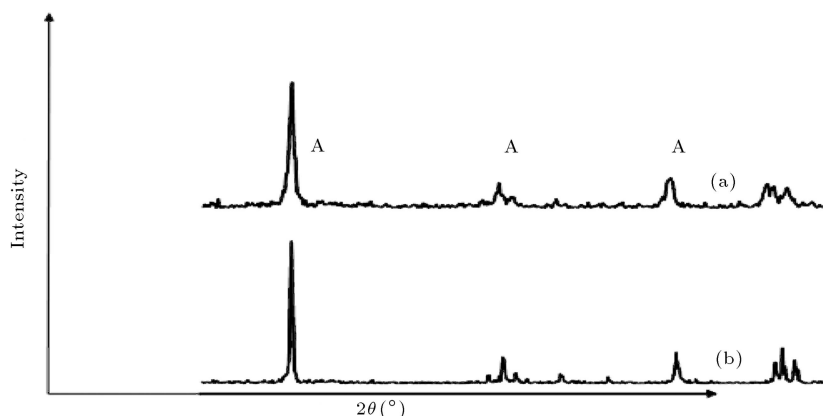


Figure 4. Powder XRD diffractogram of a) $\text{Zn}^{2+}/\text{Fe}^{3+}/\text{TiO}_2$ (0.0005: 0.0005: 1) and b) TiO_2 anatase (commercial) catalysts.

by the low quantity of dopants present in the prepared catalyst material.

CONCLUSIONS

The photocatalytic degradation of the studied VOCs is found to depend on the concentration and type of dopant ions and to the type of VOCs. It is revealed that the catalyst with optimum dopant ratio gives the highest percentage degradation of studied VOCs; an example for $\text{Zn}^{2+}/\text{Fe}^{3+}/\text{TiO}_2$ catalyst is 0.0005: 0.0005: 1. The rate of degradation of the studied chlorinated hydrocarbons follows the order: $\text{CHCl}_3 > \text{CH}_2\text{Cl}_2 > \text{CCl}_4$. Interestingly, the photocatalytic degradation pathway studies using GC-MS for VOCs are able to detect new reaction pathways for chloroform and carbon tetrachloride using $\text{Zn}^{2+}/\text{Fe}^{3+}/\text{TiO}_2$ catalyst.

ACKNOWLEDGMENTS

The authors are grateful to the Ministry of Science, Technology and Innovation, Malaysia for IRPA Vot 74248 and Universiti Teknologi Malaysia for financial support.

REFERENCES

- He, C., Xiong, Y., Chen, J. and Zhu, X. "Photoelectrochemical performance of Ag-TiO₂/ITO film and photoelectrocatalytic activity towards the oxidation of organic pollutants", *J. Photochem. Photobio. A: Chem.*, **157**, pp. 71-79 (2003).
- Brezova, V., Blazkova, A., Karpinsky, L., Groskova, J., Havlinova, B., Jorik, V. and Ceppan, M. "Phenol decomposition using Mⁿ⁺/TiO₂ photocatalysts supported by the sol-gel technique on glass fibers", *J. Photochem. Photobio. A: Chem.*, **109**, pp. 177-183 (1997).
- Yuan, Z-h., Jia, J-h. and Zhang, L-d. "Influence of co-doping of Zn (II) + Fe (III) on the photocatalytic activity of TiO₂ for phenol degradation", *Mater. Chem. Phys.*, **73**, pp. 323-326 (2002).
- Navio, J.A., Colon, G., Trillas, M., Peral, J., Domeneh, X., Testa, J.J., Padron, J., Rodriguez, D. and Litter, M.J. "Heterogeneous photocatalytic reactions of nitrite oxidation and Cr (VI) reduction on iron-doped titania prepared by the wet impregnation method", *Applied Catalysis B: Environment*, **16**, pp. 187-196 (1998).
- Arana, J., Dioz, O., Dona Rodriguez, G., Saracho, M.M., Herrera Melian, J.A. and Perez Pena, J. "Photocatalytic degradation of formic acid using Fe/TiO₂ catalysts: The role of Fe³⁺/Fe²⁺ as TiO₂ dopant ions in the degradation mechanism", *Applied Catalysis B: Environment*, **32**, pp. 49-61 (2001).
- Arroyo, R., Cordoba, G., Padilla, J. and Lara, V.H. "Influence of manganese ions on the anatase-rutile phase transition of TiO₂ prepared by sol-gel process", *Mater. Lett.*, **54**, pp. 397-420 (2002).
- Yang, P., Lu, C., Hua, N. and Du, Y. "Titanium dioxide nanoparticles co-doped with Fe³⁺ and Eu³⁺ ions for photocatalysis", *Mater. Lett.*, **57**, pp. 794-801 (2002).
- Feiyen, C., Pehkonen, S.O. and Ray, M.B. "Kinetics and mechanisms of UV-photodegradation of chlorinated organics in the gas phase", *Water Research*, **36**, pp. 4203-4214 (2002).
- Kato, K., Tsuzuki, A., Taoda, H., Torii, Y., Kto, T. and Butsugan, Y. "Crystal structures of TiO₂ thin coatings prepared from the alkoxide solution via the dip-coating technique affecting the photocatalytic decomposition of aqueous acetic acid", *J. Mater. Sci.*, **29**, pp. 5911-5915 (1994).
- Jiang, H. and Gao, L. "Enhancing the UV inducing hydrophilicity of TiO₂ thin film by doping Fe ions", *Mater. Chem. Phys.*, **77**, pp. 878-881 (2002).
- Sonawane, R.S., Kale, B.B. and Dongare, M.K. "Preparation and photo-catalytic activity of Fe-TiO₂ thin films prepared by sol-gel dip coating", *Mater. Chem. Phys.*, **85**, pp. 52-57 (2004).

APPENDICES

Appendix A

Fragments obtained before illumination of UV light for dichloromethane using $Zn^{2+}/Fe^{3+}/TiO_2$ as catalyst; analyzed by using GC-MS.

Scan 57 (1.007 min): MYB 4152.D
dichloromethane

m/z	abund.	m/z	abund.	m/z	abund.	m/z	abund.
10.15	94	20.60	4543	34.50	3157	47.35	44424
10.45	108	21.80	81	35.40	18680	48.30	19344
10.75	102	22.60	130	36.40	4962	49.30	238144
11.05	110	23.60	108	37.40	6214	50.30	9240
12.75	3177	25.05	491	38.40	1513	51.30	67432
13.75	10011	26.05	532	40.35	44032	52.20	713
14.75	192128	28.55	919360	41.35	7945	53.20	76
16.60	53560	29.55	24440	42.35	5238	54.20	53
17.70	22792	30.55	832	43.35	964	54.50	43
18.60	94128	32.40	641024	44.35	6177	55.30	93
19.70	946	33.40	809	45.35	167	56.25	156

CH_2Cl^+
 CH_3Cl^+
 $OC1^+$

Scan 57 (1.007 min): MYB 4152.D
dichloromethane

m/z	abund.	m/z	abund.	m/z	abund.	m/z	abund.
56.85	56	67.00	64	76.65	58	85.90	86896
57.95	48	67.80	63	77.25	40	86.90	2691
58.75	56	69.20	88	78.35	40	87.90	13525
59.55	41	70.10	763	78.95	31	88.85	183
60.15	64	70.70	49	79.45	55	89.95	39
61.15	74	71.30	80	80.50	62	90.95	33
62.65	59	72.00	561	81.00	44	91.15	32
63.25	57	73.95	53	81.90	1950	91.55	46
64.90	64	73.95	116	82.90	16368	92.85	51
65.40	59	74.95	33	83.90	143232	93.35	30
66.40	33	75.25	32	84.90	12404	93.95	31

CH_2ClO^+

CCl_2^+

Scan 57 (1.007 min): MYB 4152.D
dichloromethane

m/z	abund.	m/z	abund.	m/z	abund.	m/z	abund.
94.75	43	100.90	34	108.45	26	118.60	193
95.35	42	101.60	30	109.85	21	119.60	277
95.85	49	102.70	31	111.05	24	120.65	58
96.30	36	103.20	31	111.85	38	121.55	127
96.90	59	104.10	24	112.50	24	122.75	36
97.70	44	105.25	45	113.80	30	123.25	25
98.80	61	105.85	28	114.30	50	123.65	22
99.40	26	107.35	32	115.70	32	124.35	22
100.00	45	107.65	27	115.90	37	125.05	21
100.30	30	107.95	26	116.60	157	125.85	35
100.60	32	108.25	27	117.60	283	126.05	31

$CHCl_2O^+$

$COCl_2^+$

$CHCl_2^+$

CCl_3^+

Scan 57 (1.007 min): XYB 4152.D
dichloromethane

m/z	abund.	m/z	abund.	m/z	abund.	m/z	abund.
126.35	30	135.50	20	146.00	43	156.05	30
126.62	30	135.70	27	147.40	33	160.15	20
126.85	28	117.15	26	149.80	23	160.75	26
127.66	29	128.25	11	180.70	29	161.80	27
128.25	28	139.05	25	151.20	21	163.00	33
129.00	30	139.35	20	153.55	25	163.60	22
129.40	49	140.35	27	154.15	23	163.80	22
131.00	25	141.15	28	154.95	24	164.20	24
131.60	21	141.45	23	155.35	28	165.80	36
133.00	33	142.45	37	156.45	21	167.10	25
134.00	34	143.75	29	156.65	21	167.40	21

$CHCl_2OO^+$

Scan 57 (1.007 min): MYB 4152.D
dichloromethane

m/z	abund.	m/z	abund.	m/z	abund.	m/z	abund.
168.00	25	185.85	20	199.70	23	220.25	22
168.60	27	186.95	29	201.10	20	222.95	42
169.85	40	187.75	22	201.25	20	229.00	32
174.65	23	190.05	29	203.15	30	229.60	23
177.40	24	191.55	22	205.75	60	231.10	30

Appendix B

Fragments obtained after illumination of UV light for dichloromethane using $Zn^{2+}/Fe^{3+}/TiO_2$ as catalyst; analyzed by using GC-MS.

Scan 57 (1.008 min): MYB 4167.D

dichloromethane							
m/z	abund.	m/z	abund.	m/z	abund.	m/z	abund.
10.35	104	21.30	77	30.55	923	44.35	6860
10.65	94	21.80	44	32.50	623872	45.35	156
11.25	122	22.10	38	34.50	3314	47.35	37944
12.75	3758	22.70	83	35.40	17160	48.30	18520
13.85	8731	23.20	54	36.40	4520	49.30	225472 → CH ₂ Cl ⁺
14.75	211840	23.50	65	37.40	5801	50.30	8133 → CH ₃ Cl ⁺
16.60	52992	23.70	65	38.40	1473	51.30	57600 → OCl ⁺
17.70	20912	24.25	107	40.35	46984	52.20	702
18.70	93224	25.05	462	41.35	7037	52.90	47
19.70	966	28.55	880192	42.35	4703	53.40	44
20.60	4437	29.55	22456	43.35	777	54.00	54

Scan 57 (1.008 min): MYB 4167.D

dichloromethane							
m/z	abund.	m/z	abund.	m/z	abund.	m/z	abund.
55.60	82	61.55	41	68.00	59	77.15	47
56.35	104	62.25	38	69.20	89	77.75	25
57.15	46	62.45	38	70.10	653	78.55	30
57.75	27	63.05	74	71.00	74	79.15	38
58.15	40	63.75	54	72.00	428	79.45	39
58.65	49	64.40	46	73.15	65	79.95	48
58.95	55	65.00	53	73.95	130	81.90	1810 → CCl ₂ ⁺
59.15	46	65.50	26	74.85	41	82.90	15626 → CHCl ₂ ⁺
59.95	68	66.10	34	75.35	30	83.90	128688
60.45	51	66.70	43	75.85	45	84.90	11414
61.05	52	67.00	48	85.90	48	85.90	79536

Scan 57 (1.008 min): MYB 4167.D

dichloromethane							
m/z	abund.	m/z	abund.	m/z	abund.	m/z	abund.
86.90	2604	94.75	66	102.60	38	111.25	31
87.90	11767	96.15	58	103.20	37	112.35	41
88.85	165	96.80	85	103.80	22	113.50	31
90.15	35	97.60	37	104.10	23	114.20	40
90.85	25	97.90	35	104.55	32	115.60	34 → CHCl ₂ OO ⁺
91.65	25	98.90	62	105.05	26	116.60	177
91.95	23	99.80	49	106.55	50	117.60	260
92.25	28	100.90	24	107.15	29	118.60	144 → CCl ₃ ⁺
92.45	26	101.10	24	109.95	26	119.60	224
92.85	31	101.50	28	110.25	21	120.55	52
93.65	22	102.30	39	110.55	21	121.55	113

Scan 57 (1.008 min): MYB 4167.D

dichloromethane							
m/z	abund.	m/z	abund.	m/z	abund.	m/z	abund.
122.45	29	133.00	27	145.20	27	158.35	21
123.45	23	133.20	26	148.50	28	159.05	30
124.15	23	133.60	32	149.30	22	159.55	21
125.45	35	134.30	22	150.60	30	160.45	28
126.15	22	135.70	23	151.30	34	161.90	26
127.45	41	136.30	23	152.20	34	162.10	28
128.15	29	137.05	29	152.85	27	162.80	24
128.70	26	137.35	36	154.95	22	165.00	31
129.50	46	137.55	28	156.05	31	165.70	20
130.30	24	140.25	22	157.15	23	168.40	20
131.50	47	140.85	21	158.05	22	168.70	21

Scan 57 (1.008 min): MYB 4167.D

dichloromethane							
m/z	abund.	m/z	abund.	m/z	abund.	m/z	abund.
169.85	22	182.80	23	198.80	21	242.50	24
170.15	26	183.70	27	205.75	51	245.80	20
171.15	28	184.50	23	206.85	23		
172.05	36	184.70	24	209.90	28		
173.05	25	187.15	34	212.00	20		

Appendix C

Fragments obtained before illumination of UV light for chloroform using $Zn^{2+}/Fe^{3+}/TiO_2$ as catalyst; analyzed by using GC-MS.

Scan 57 (1.008 min): MYB 4167.D

dichloromethane							
m/z	abund.	m/z	abund.	m/z	abund.	m/z	abund.
10.35	104	21.30	77	30.55	923	44.35	6860
10.65	94	21.80	44	32.50	623872	45.35	156
11.25	122	22.10	38	34.50	3314	47.35	37944
12.75	3758	22.70	83	35.40	17160	48.30	18520
13.85	8731	23.20	54	36.40	4520	49.30	225472 → CH ₂ Cl ⁺
14.75	211604	23.50	65	37.40	5801	50.30	8133 → CH ₃ Cl ⁺
16.60	52992	23.70	65	38.40	1473	51.30	57600 → OCl ⁺
17.70	20912	24.25	107	40.35	46984	52.20	702
18.70	93224	25.05	462	41.35	7037	52.90	47
19.70	966	28.55	880192	42.35	4703	53.40	44
20.60	4437	29.55	22456	43.35	777	54.00	54

Scan 57 (1.008 min): MYB 4167.D

dichloromethane							
m/z	abund.	m/z	abund.	m/z	abund.	m/z	abund.
55.60	82	61.55	41	68.00	59	77.15	47
56.35	104	62.25	38	69.20	89	77.75	25
57.15	46	62.45	38	70.10	653	78.55	30
57.75	27	63.05	74	71.00	74	79.15	38
58.15	40	63.75	54	72.00	428	79.45	39
58.65	49	64.40	46	73.15	65	79.95	48
58.95	55	65.00	53	73.95	130	81.90	1810
59.15	46	65.50	26	74.85	41	82.90	15626 → CCl ₂ ⁺
59.95	68	66.10	34	75.35	30	83.90	128688 → CHCl ₂ ⁺
60.45	51	66.70	43	75.85	45	84.90	11414
61.05	52	67.00	48	85.90	79536		

Scan 57 (1.008 min): MYB 4167.D

dichloromethane							
m/z	abund.	m/z	abund.	m/z	abund.	m/z	abund.
86.90	2604	94.75	66	102.60	38	111.25	31
87.90	11767	96.15	58	103.20	37	112.35	41
88.85	165	96.80	85	103.80	22	113.50	31
90.15	35	97.60	37	104.10	23	114.20	0
90.85	25	97.90	35	104.55	32	115.60	34 → CHCl ₂ OO ⁺
91.65	25	98.90	62	105.05	26	116.60	117
91.95	23	99.80	49	106.55	50	117.60	260
92.25	28	100.90	24	107.15	29	118.60	144 → CCl ₃ ⁺
92.45	26	101.10	24	109.95	26	119.60	224
92.85	31	101.50	28	110.25	21	120.55	52
93.65	22	102.30	39	110.55	21	121.55	113

Scan 57 (1.008 min): MYB 4167.D

dichloromethane							
m/z	abund.	m/z	abund.	m/z	abund.	m/z	abund.
122.45	29	133.00	27	145.20	27	158.35	21
123.45	23	133.20	26	148.50	28	159.05	30
124.15	23	133.60	32	149.30	22	159.55	21
125.45	35	134.30	22	150.60	30	160.45	28
126.15	22	135.70	23	151.30	34	161.90	26
127.45	41	136.30	23	152.20	34	162.10	28
128.15	29	137.05	29	152.85	27	162.80	24
129.50	46	137.55	28	156.05	31	165.70	20
130.30	24	140.25	22	157.15	23	168.40	20
131.50	47	140.85	21	158.05	22	168.70	21

Scan 57 (1.008 min): MYB 4167.D

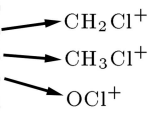
dichloromethane							
m/z	abund.	m/z	abund.	m/z	abund.	m/z	abund.
169.85	22	182.80	23	198.80	21	242.50	24
170.15	26	183.70	27	205.75	51	245.80	20
171.15	28	184.50	23	206.85	23		
172.05	36	184.70	24	209.90	28		
173.05	25	187.15	34	212.00	20		

Appendix D

Fragments obtained after illumination of UV light for chloroform using $Zn^{2+}/Fe^{3+}/TiO_2$ as catalyst, analyzed by using GC-MS.

Scan 57 (1.012 min): MYB 4087C.D
chloroform

m/z	abund.	m/z	abund.	m/z	abund.	m/z	abund.
10.85	99	22.60	117	36.40	4079	47.25	57888
11.75	217	23.50	71	37.40	6033	48.20	21840
12.75	3490	24.45	116	38.40	1245	49.20	18000
13.75	10952	25.15	133	40.35	43720	50.20	7896
14.75	179840	28.55	916416	41.35	657	51.20	189
16.60	62472	29.55	31480	41.85	697	52.40	63
17.60	127280	30.55	1184	42.35	588	53.20	23
18.60	557312	32.40	632768	42.75	591	54.50	46
19.60	4814	33.40	1486	43.35	345	54.80	49
20.60	5045	34.40	3315	44.35	7615	55.10	47
21.90	67	35.40	19656	45.35	409	55.40	51



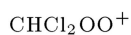
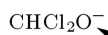
Scan 57 (1.012 min): MYB 14087C.D
chloroform

m/z	abund.	m/z	abund.	m/z	abund.	m/z	abund.
56.15	74	63.15	101	73.15	68	85.90	2306
57.05	52	64.20	29	73.95	251	86.90	20432
57.55	57	65.00	53	75.05	50	87.90	237
58.35	140	66.20	27	76.25	28	88.65	37
58.55	132	67.80	44	76.95	141	89.15	23
59.65	138	68.80	67	77.95	36	89.75	29
60.15	57	69.10	70	78.95	39	90.25	36
60.45	62	70.10	1303	81.90	8285	91.05	20
61.45	30	71.20	70	82.90	221568	91.25	21
62.25	57	72.00	1065	83.90	7833	91.55	21
62.55	64	72.95	66	84.90	135936	92.25	24



Scan 57 (1.012 min): MYB 14087C.D
chloroform

m/z	abund.	m/z	abund.	m/z	abund.	m/z	abund.
92.95	27	100.40	23	110.85	25	122.62	111
93.95	33	100.90	57	111.45	31	123.55	179
94.75	28	102.10	33	112.40	40	124.25	23
95.95	85	102.80	38	113.70	28	124.55	38
96.40	24	104.10	27	115.50	25	126.15	45
96.60	24	104.95	23	116.60	2250	126.75	28
97.10	25	107.05	24	117.60	4129	127.55	29
97.60	26	107.65	20	118.60	2280	128.25	30
98.10	29	108.85	39	119.60	3814	129.50	44
99.20	26	109.05	33	120.55	730	129.70	44
99.90	36	109.95	26	121.55	1206	130.10	22



Scan 57 (1.012 min): MYB 14087C.D
chloroform

m/z	abund.	m/z	abund.	m/z	abund.	m/z	abund.
130.40	22	148.60	23	166.40	23	192.05	29
131.30	33	148.90	27	169.15	32	192.75	20
133.10	23	149.70	24	171.85	27	193.60	27
133.70	31	150.50	24	174.45	20	198.00	23
135.80	24	153.55	32	178.00	24	198.90	21
136.85	28	154.35	23	179.10	28	199.80	20
138.15	26	156.95	39	184.40	31	201.45	22
140.75	24	157.55	27	186.55	25	203.75	25
140.95	24	159.05	28	189.25	26	205.85	87
144.90	30	159.65	20	189.55	22	207.05	36
147.80	24	163.10	20	190.15	26	209.15	22



Scan 57 (1.012 min): MYB 14087C.D
chloroform

m/z	abund.	m/z	abund.	m/z	abund.
211.10	21				
213.00	28				
216.80	22				
219.65	20				
220.45	43				

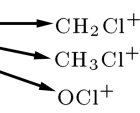
Appendix E

Fragments obtained before illumination of UV light for carbon tetrachloride using $Zn^{2+}/Fe^{3+}/TiO_2$ as catalyst, analyzed by using GC-MS.

Scan 57 (1.012 min): MYB 4087C.D

chloroform

m/z	abund.	m/z	abund.	m/z	abund.	m/z	abund.
10.85	99	22.60	117	36.40	4079	47.25	57888
11.75	217	23.50	71	37.40	6033	47.20	21840
12.75	3490	24.45	116	38.40	1245	49.20	18000
13.75	10952	25.15	133	40.35	43720	50.20	7896
14.75	179840	28.55	916416	41.35	657	51.20	189
16.60	62472	29.55	31480	41.85	697	52.40	63
17.60	127280	30.55	1184	42.35	588	53.20	23
18.60	557312	32.40	632768	42.75	591	54.50	46
19.60	4814	33.40	1486	43.35	345	54.80	49
20.60	5045	34.40	3315	44.35	7615	55.10	47
21.90	67	35.40	19656	45.35	409	55.40	51



Scan 57 (1.012 min): MYB 4087C.D

chloroform

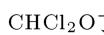
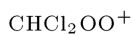
m/z	abund.	m/z	abund.	m/z	abund.	m/z	abund.
56.15	74	63.15	101	73.15	68	85.90	2306
57.05	52	64.20	29	73.95	251	86.90	20432
57.55	57	65.00	53	75.05	50	87.90	237
58.35	140	66.20	27	76.25	28	88.65	37
58.55	132	67.80	44	76.95	141	89.15	23
59.65	138	68.80	67	77.95	36	89.75	29
60.15	57	69.10	70	78.95	39	90.25	36
60.45	62	70.10	1303	81.90	8285	91.05	20
61.45	30	71.20	70	82.90	221568	91.25	21
62.25	57	72.00	1065	83.90	7833	91.55	21
62.55	64	72.95	66	84.90	135936	92.25	24



Scan 57 (1.012 min): MYB 4087C.D

chloroform

m/z	abund.	m/z	abund.	m/z	abund.	m/z	abund.
92.95	27	100.40	23	110.85	25	122.65	111
93.95	33	100.90	57	111.45	31	123.55	179
94.75	28	102.10	33	112.40	40	124.25	23
95.95	85	102.80	38	113.70	28	124.55	38
96.40	24	104.10	27	115.50	25	126.15	45
96.60	24	104.95	23	116.60	2250	126.75	28
97.10	25	107.05	24	117.60	4129	127.55	29
97.60	26	107.65	20	118.60	2280	128.25	30
98.10	29	108.85	39	119.60	3814	129.50	44
99.20	26	109.05	33	120.55	730	129.70	44
99.90	36	109.95	26	121.55	1206	230.10	22



Scan 57 (1.012 min): MYB 4087C.D

chloroform

m/z	abund.	m/z	abund.	m/z	abund.	m/z	abund.
130.40	22	148.60	23	166.60	23	192.05	29
131.30	33	148.90	27	169.15	32	192.75	20
133.10	23	149.70	24	171.85	27	193.60	27
133.70	31	150.50	24	174.45	20	198.00	23
135.80	24	153.55	32	178.00	24	198.90	21
136.85	28	154.35	23	179.10	28	199.80	20
138.15	26	156.95	39	184.40	31	201.45	22
140.75	24	157.55	27	186.55	25	203.75	25
140.95	24	159.05	28	189.25	26	205.85	87
144.90	30	159.65	20	189.55	22	207.05	36
147.80	24	163.10	20	190.15	26	209.15	22

Scan 57 (1.012 min): MYB 4087C.D

chloroform

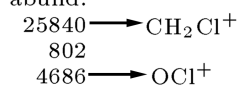
m/z	abund.	m/z	abund.	m/z	abund.	m/z	abund.
211.10	21						
213.00	28						
216.80	22						
219.65	20						
220.45	43						

Appendix F

Fragments obtained after illumination of UV light for carbon tetrachloride using $Zn^{2+}/Fe^{3+}/TiO_2$ as catalyst, analyzed by using GC-MS.

Scan 59 (1.036 min): MYB 4200.D
carbon tetrachloride

m/z	abund.	m/z	abund.	m/z	abund.	m/z	abund.
10.15	75	21.40	65	36.40	2816	49.30	25840
10.45	64	22.60	104	37.40	7848	50.30	802
10.75	81	23.30	87	38.40	890	51.20	4686
10.95	79	24.35	64	40.35	38440	52.30	91
12.75	4224	25.05	112	41.35	1258	52.90	48
14.75	142144	28.55	883776	42.35	1061	53.20	56
16.70	43416	29.55	20160	43.35	457	54.30	38
17.70	19440	30.55	618	44.35	6046	54.60	38
18.70	85000	32.50	556864	45.45	119	55.50	36
19.60	463	34.50	2656	47.35	42736	55.90	34
20.60	3888	35.40	24592	48.30	2066	56.05	34



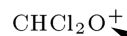
Scan 59 (1.036 min): MYB 4200.D
carbon tetrachloride

m/z	abund.	m/z	abund.	m/z	abund.	m/z	abund.
56.45	47	66.00	32	77.05	38	87.90	959
56.65	43	66.50	26	77.45	29	88.55	27
57.35	62	67.50	20	78.95	30	91.25	27
58.65	3135	68.60	39	79.75	30	92.55	22
59.65	3322	70.10	1657	79.95	26	93.95	23
60.65	904	71.00	34	81.90	37736	94.95	30
61.55	110	72.10	1088	82.90	2458	96.25	24
62.25	52	73.95	168	83.90	33840	96.70	21
63.15	362	74.75	28	84.90	1714	97.60	37
64.20	31	75.55	47	85.90	98.77	98.30	20
65.20	116	76.05	21	87.00	325	99.40	35



Scan 59 (1.036 min): MYB 4200.D
carbon tetrachloride

m/z	abund.	m/z	abund.	m/z	abund.	m/z	abund.
100.00	25	112.15	22	123.55	88	141.85	25
102.00	31	112.40	25	124.35	36	143.45	22
102.60	31	112.60	23	125.95	21	144.45	21
103.60	32	113.40	30	127.25	24	145.30	29
104.10	25	114.20	49	129.60	26	145.90	22
104.85	22	116.60	173184	131.00	22	148.20	23
105.05	21	118.60	168000	134.20	34	150.10	27
105.75	27	119.60	1985	135.60	25	151.20	22
106.65	21	120.55	51200	135.90	20	151.40	23
107.75	28	121.55	628	136.10	22	154.15	22
108.45	26	122.55	4902	138.55	25	156.75	33



Scan 59 (1.036 min): MYB 4200.D
carbon tetrachloride

m/z	abund.	m/z	abund.	m/z	abund.	m/z	abund.
158.15	23	230.960	21				
163.10	24	232.70	22				
185.25	20	233.45	28				
195.50	23	234.35	21				
196.10	23	247.20	22				
201.45	29						
202.15	28						
205.75	47						
217.35	29						
224.15	24						
227.00	21						



BIOGRAPHIES

Wan Azelee Wan Abu Bakar was born in 1959 in Kelantan, Malaysia. After graduation from the Department of Chemistry at the National University of Malaysia in 1983, he continued his studies into heterogeneous catalysis at Nottingham University, in England, and received his PhD in 1995. He then joined Universiti Teknologi Malaysia, where he is presently a Professor of Inorganic Chemistry. Professor Wan Azelee Wan Abu Bakar is the author of 100 papers published in national and international journals and 4 chemistry text books for university students.

Rusmidah Ali was born in 1957 in Klang, Selangor, in Malaysia. She obtained her BS degree in Chemistry in 1980 from Universiti Kebangsaan Malaysia, and then

received her MS and PhD degrees from Southampton University, in the UK, in 1983 and 1987, respectively. She then joined Universiti Teknologi Malaysia, where she is presently Associate Professor of Inorganic Chemistry. She is author of 30 papers published in national and international journals and 11 books.

Mohd Yusuf Othman was born in 1952 in Pahang, Malaysia. After graduation from Universiti Kebangsaan Malaysia in 1975, he continued his studies at University College, Swansea at the University of Wales, receiving his MS and PhD degrees in 1978 and 1985, respectively. He then joined Universiti Teknologi Malaysia and became an Associate Professor in the Department of Chemistry in 1991. He is author of 20 papers published in national and international journals.